Cycling phosphorus on the Archean Earth: Part I. Continental weathering and riverine transport of phosphorus

Jihua Hao, Andrew H. Knoll, Fang Huang, Robert M. Hazen, Isabelle Daniel

Cycling Phosphorus on the Archean Earth: Part I. Continental weathering and riverine transport of phosphorus

Author: Jihua Hao[1,2*], Andrew H. Knoll[3], Fang Huang[4], Robert M. Hazen[5], Isabelle Daniel[1]

*Corresponding author: haojihua@gmail.com

[1]Univ Lyon, Université Lyon 1, Ens de Lyon, CNRS, UMR 5276 LGL-TPE, F-69622, Villeurbanne, France

[2]Present: Department of Marine and Coastal Sciences, Rutgers University, New Brunswick NJ 08901, USA.

[3]Department of Organismic and Evolutionary Biology, Harvard University, Cambridge MA 02138, USA

[4]Tetherless World Constellation, Rensselaer Polytechnic Institute, Troy NY, 12180, USA

[5]Geophysical Laboratory, Carnegie Institution for Science, Washington DC, 20015, USA

Abstract:

Phosphorus (P) is the key nutrient thought to limit primary productivity on geological timescales. Phosphate levels in Archean marine sediments are low, but quantification of the P cycle and how it changed through a billion years of recorded Archean history remain a challenge, hindering our understanding of the role played by P in biosphere/geosphere co-evolution on the early Earth.

Here, we design kinetic and thermodynamic models to quantitatively assess one key component of the early P cycle – continental weathering – by considering the emergence and elevation of continents, as well as the evolution of climate, the atmosphere, and the absence of macroscopic vegetation during the Archean Eon. Our results suggest that the weathering rate of apatite, the major P-hosting mineral in the rocks, was at least five times higher in the Archean Eon than today, attributable to high levels of $pCO_{2,g}$. Despite this, the weathering flux of P to the oceans was negligible in the early Archean Eon, increasing to a level comparable to or greater than the modern by the end of eon, a consequence of accelerating continental emergence. Furthermore, our thermodynamic calculations indicate high solubilities of primary and secondary P-hosting minerals in the acidic weathering fluids on land, linking to high Archean $pCO_{2,g}$. Thus, weathering of P was both kinetically and thermodynamically favorable on the Archean Earth, and river water could transport high levels of dissolved P to the oceans, as also supported by the observed P-depletion in our new compilation of Archean paleosols. Lastly, we evaluated the relative rates of physical erosion and chemical weathering of silicates during the Archean Eon. The results suggest that continental weathering on the early and middle Archean Earth might have been transport-limited due to low erosion rates associated with limited subaerial emergence and low plateau elevations; by the late Archean, however, continental weathering would have transited to kinetically-limited state because of continental emergence, increased plateau elevation, and

weakening weathering rates. Overall, our weathering calculations together with paleosol evidence indicate an increasing flux of bioavailable P to the oceans through time, associated with late Archean continental emergence, reaching levels comparable to or higher than modern values by the end of the eon. Increased P fluxes could have fueled increasing rates of primary production, including oxygenic photosynthesis, through time, facilitating the irreversible oxidation of the Earth's atmosphere early in the Proterozoic Eon. (388 words)

Keywords: phosphorus; emergence of land; elevation of land; physical erosion; chemical weathering; paleosols (6/6)

1. Introduction

Phosphorus (P) is an essential bionutrient. Critical to the genetic material (nucleotides), membranes (phospholipids) and energy transfer (ATP) in cells, its availability is thought to limit primary productivity on geological timescales (Laakso and Schrag, 2018; Ruttenberg, 2013; Tyrrell, 1999). Temporal variations in the P content of sedimentary rocks such as iron formation and carbonaceous shale suggest low levels of phosphate in Archean marine sediments (Bjerrum and Canfield, 2002; Planavsky et al., 2010; Reinhard et al., 2017), but quantification of the P cycle and how it changed through a billion years of recorded Archean history remain a challenge, hindering our understanding of the role played by P in biosphere/geosphere co-evolution on the early Earth.

The modern P cycle involves two dominant phosphate sources to the sunlit ocean: continental weathering and recycling in the oceans. Continental weathering provides the ultimate source of bio-available P to marine ecosystems, but due to the highly efficient recycling of organic matter in the modern oxidizing ocean, the flux of recycled P exceeds the continental input of P by two to three orders of magnitude (Schlesinger and Bernhardt, 2013). Thus, the high primary productivity of the modern ocean is sustained predominantly by recycled P. P burial on the other hand is determined by P input from continental weathering. On the early Earth, before the oxygenation of the atmosphere and ocean, recycling of organics in anoxic seawater might have been suppressed by a limited supply of oxidants (O_2, sulfate, nitrate, and ferric iron) (Kipp and Stüeken, 2017; Laakso and Schrag, 2018), and P released to subsurface water masses might have been sequestered by reaction with ferrous iron to form vivianite (Derry, 2015). As a consequence, continental weathering might have accounted for a relatively larger proportion of total P supplied to primary producers in Archean oceans.

Continental input of P into early oceans, however, is poorly understood, for two major reasons. On the one hand, continental weathering of P might have been limited by less extensive subaerial exposure of land and low elevations (Flament et al., 2013; Korenaga et al., 2017; Rey and Coltice, 2008), as well as a lower P content of early igneous rocks (Cox et al., 2018). On the other hand, high levels of atmospheric $CO_{2,g}$ thought to characterize the early Earth favor weathering and riverine transport of phosphorus (Hao et al., 2017a). In addition, the absence of macroscopic vegetation on Archean continents should also have affected both chemical and physical weathering relative to the modern Earth.

Despite these challenges, there have been a few attempts to estimate the continental flux of P into Archean oceans. Hao et al. (2017a) used a thermodynamic model to simulate the maximum solubilities of apatite ($Ca_5(PO_4)_3(OH,F,Cl)$), the major P-hosted mineral in the crust, in proposed Archean weathering fluids; however, they could not quantify continental fluxes because they lacked terms for weathering kinetics, the growth and elevation of continental land, and the evolution of climate and atmosphere. Recent studies have placed constraints on the parameters that collectively govern these fluxes, including continental emergence *per se* (Flament et al., 2013; Korenaga et al., 2017), atmospheric composition (Krissansen-Totton et al., 2018), and temperature (Krissansen-Totton et al., 2018). Despite uncertainties, these estimates enable us, for the first time, to quantify continental input of bioavailable P to Archean oceans. Here we design kinetic and thermodynamic models to estimate the continental weathering of apatite and riverine transport of P, incorporating the emergence and elevation of continental land, atmospheric composition, climate, and the absence of vegetation.

2. Important environmental parameters controlling phosphorus weathering

Continental weathering of phosphorus depends on a number of environmental factors, all of which have evolved through the Earth history.

2.1 Emergence of land

Although the volume of continental crust might have increased more or less continually early in Earth history (Hawkesworth and Kemp, 2006; Roberts and Spencer, 2015), only limited evidence exists for emergent land before the middle Archean Eon. Various lines of evidence, including stratigraphic observations, geophysical simulations, and geochemical data agree that the early and middle Archean continents had only limited subaerial exposure (Arndt, 1999; Campbell and Davies, 2017; Ernst et al., 2016; Flament et al., 2013, 2008; Korenaga et al., 2017; Kump and Barley, 2007; Molnar, 2018; Trower and Lowe, 2016).

For example, the 3.5-3.26 Ga Onverwacht Group, South Africa, contains some ten kilometers of stratigraphy, but nearly all of it is volcanic, and much consists of pillow basalts extruded below sea level (Lowe and Byerly, 1999). With one exception, detrital zircons suggest that such clastic sedimentary rocks as are preserved derive largely from regional volcanics (Drabon et al., 2017). The exception is a three meter sandstone bed near the top of the Onverwacht succession that contains zircons older than 3.8 Ga. These suggest that older differentiated crust existed but was rarely eroded (Byerly et al., 2018). Clastic sedimentary rocks are more abundant in the 3.26-3.22 Ga Fig Tree Group, but the lithic grains that dominate these lithologies again speak to reworking of regional volcanics (Nocita, 1989). Only with deposition of the immediately overlying Moodies Group do we see accumulations of quartz-rich sandstones derived from exposed continental crust. Later Archean basins increase in lateral dimensions, culminating in the latest Archean Transvaal basin, whose spatial scale suggests accumulation along the margin of a large, stable craton (Knoll and

Beukes, 2009). Similar features characterize Archean stratigraphy in Western Australia (e.g., van Kranendonk, 2006).

Geochemical data also support late emergence models. End-Archean increase in the $^{87}Sr/^{86}Sr$ of carbonate rocks was originally thought to reflect continental growth (Taylor and McLennan, 1985) or continental igneous rock composition (Bataille et al., 2017), but is equally well explained in terms of late continental emergence (Flament et al., 2013; see also Pons et al., 2013, for a comparable perspective based on Zn isotopes). Indeed, interpretation in terms of emergence helps greatly to reconcile otherwise conflicting stratigraphic and geochemical inferences about continental growth on the Archean Earth. Consistent with this view, Bindeman et al. (2018) and Spencer et al. (2019) have both interpreted the oxygen isotope record in terms of late Archean continental emergence, while Kump and Barley (2007) have argued for an increase in subaerial volcanism near the Archean-Proterozoic boundary. We know of no comparable suite of evidence favoring much earlier emergence of stable continents.

Lee et al. (2018) recently proposed a scenario in which pronounced continental emergence developed only near the end of the Proterozoic Eon, catalyzing late Neoproterozoic climatic and redox transformations. This proposal is at odds with several lines of geochemical evidence documenting large continental weathering and erosional fluxes by late Archean times (Bindeman et al., 2018; Satkoski et al., 2016; Viehmann et al., 2018), not to mention thousands of meters of quartzose sandstones in earlier Proterozoic basins around the world. If all land were submerged, there would be no depletion of P during seafloor weathering, which is inconsistent with Archean paleosol records (**Fig. 6**). Moreover, in the warm climate suggested by biogeochemical models for a land-free Archean (Krissansen-Totton et al., 2018), rapid precipitation of vivianite would remove essentially all available P from seawater. Thus, any scenario with essentially no exposed land mass implies

157 minimal global primary production sustained by limited fluxes of P from extraterrestrial
158 sources (Pasek and Lauretta, 2008; Tsukamoto et al., 2018), inconsistent with evidence for
159 substantial biological activity in the Archean ocean. Taken together, sedimentary and
160 geochemical evidence make protracted late Archean continental emergence a more plausible
161 scenario.

162 Quantification of continental emergence depends on a number of parameters, none of
163 them well constrained. These include mantle temperature, crustal composition – and hence
164 buoyancy, seawater volume, modes and rates of tectonic activity, and continental hypsometry
165 (Korenaga et al., 2017). Previous studies of the Archean Earth have rarely incorporated all of
166 these parameters; indeed, parameter selection has commonly seemed arbitrary. For this paper,
167 we chose three models for secular change in continental emergence from two recent studies
168 (**Fig. 1a**) (Flament et al., 2013; Korenaga et al., 2017). Among the available estimates, we
169 suggest that these provide the best understanding of continental emergence available at
170 present. Moreover, because they incorporate multiple models of continental growth and
171 mantle devolatilization/revolatilization, these papers provide a broad range of possible
172 histories.

173 Apart from more limited emergence of the Archean continents, a hotter and more
174 buoyant Archean mantle could not support high plateau elevations (Fig. 1b; Flament et al.,
175 2013; Rey and Coltice, 2008), although the actual elevation should depend on a balance
176 between tectonic uplifting and exhumation/erosion. Based on the classic Culling's model
177 (Culling 1960, 1963), the erosion rates is linearly proportional to topographic slope, which
178 depends on relative elevation. Physical erosion is responsible for the removal of sediment and
179 exposure of fresh rock surface for chemical weathering. We further simplify Culling's model
180 by assuming that physical erosion is proportional to the elevation of land, i.e., $E_r \propto H$, an
181 approach that has previously been applied to macroscale erosion processes (Lee et al., 2015;

Jadamec et al., 2007). Thus, physical erosion on the Archean Earth was probably limited by the low elevation of continental land, as well as its limited aerial extent, as investigated below.

2.2 P content of rocks

The P content of erodible rocks is another important factor in estimating the weathering flux of P. P content depends on rock composition (Porder and Ramachandran, 2013; Ronov, 1982) and exposure through geological time (Cox et al., 2018). On the modern Earth, the exposure area of sedimentary rocks exceeds that of volcanics (Bluth & Kump, 1991). Thus, on the modern Earth, the contribution of sedimentary rock weathering to continental P flux can potentially be substantial (Hartmann et al., 2014). On the early Archean, however, this sedimentary reservoir might have been less important. The P content of sedimentary rocks varies widely and can be either higher or lower than that of ultramafic-mafic volcanic rocks (Porder & Ramachandran, 2013; Ronov, 1982), which were the major crustal lithologies in the Archean Eon. Quantification of the contribution of sedimentary rock weathering to P flux needs to consider relative P content, surface exposure, and weathering kinetics of sedimentary vs. volcanic rocks. Collectively, the resultant uncertainty may become too large to yield any useful implications. It is also possible that agpaitic rocks, which are unusually rich in phosphorus, could add complexity to weathering and erosional P fluxes; however, all known examples of agpaitic rocks postdate the Archean (Marks and Markl, 2017). With these unknowns and uncertainties in mind, we instead chose to use relative P content of crust in the Archean and modern Earth. A compilation of more than 176,000 igneous rock samples indicates that the P content of the Archean crust was perhaps half that estimated for today, although felsic rocks show no pronounced secular trend (Cox et al., 2018).

2.3 Archean atmospheric composition

Acidity and redox state are two more important controls on the chemical dissolution of phosphorus. Rainwater acidity is controlled by the dissolution of atmospheric CO_2 and deprotonation of H_2CO_3. It has been generally proposed that high levels of CO_2 are required to compensate the weaker young sun (20 to 30 % lower luminosity) (Gough, 1981) and sustain a temperate climate in the Archean. As a result, Archean rainwater is estimated to have been more acidic than modern (Hao et al., 2017a). Log dissolution rate of the major P-hosted minerals, i.e. apatite, has been experimentally shown to increase linearly with decreasing pH (Guidry and Mackenzie, 2003). The solubility limits of P-minerals also depend significantly on pH, as investigated below.

The redox state of the Archean atmosphere and surface waters is thought to have been weakly reducing (Hao et al., 2019). Under these conditions, ferrous iron is stable rather than the ferric iron that generally forms in modern oxidizing weathering reactions. Given the much greater solubility of ferrous iron relative to ferric iron, Archean weathering should result in Fe-depletion, as evidenced by the paleosol record (Rye and Holland, 1998) and thermodynamic simulation (Hao et al., 2017b). Today, the largest proportion of the reactive phosphorus pool in riverine transport is Fe-bound phosphorus, because during oxidative weathering Fe(II) is oxidized to Fe(III), leading to the formation of Fe(III)-(hydr)oxide or Fe(III)-coated clay minerals that have a high surface adsorption affinity for phosphate (House, 2003; Withers and Jarvie, 2008). This surface retention of P is thought to be a key process limiting dissolved P levels in modern river water. However, we expect there would have been little Fe-bound inorganic phosphate in anoxic Archean river water and, correspondingly, high concentrations of dissolved inorganic phosphate. Below we examine whether or not the acidic and anoxic weathering fluids could transport high concentrations of dissolved phosphate on the Archean Earth.

232

233 *2.4 Absence of vegetation*

234 The presence of land plants affects both chemical weathering and physical erosion.
235 On the one hand, vegetation is thought to facilitate chemical weathering through the secretion
236 of organic ligands that attack primary minerals (Neaman et al., 2005) and/or elevation of soil
237 $pCO_{2,g}$ by means of microbial decomposition of organic debris in the soil (Berner, 2004).
238 Overall, the presence of non-microbial vegetation is proposed to accelerate the chemical
239 dissolution of primary minerals by a factor of 3 to 4, as calculated by cation release from
240 vegetated vs. barren areas (Berner et al., 2004). The enhancing factor of 4 is further supported
241 by attempts to match the COPSE model to multiple Phanerozoic paleo-weathering proxies
242 (Lenton et al., 2018). On the other hand, vegetation can protect substrates from physical
243 erosion and thus hinder the exposure of fresh rock for further weathering, particularly where
244 removal of the soil cover is not efficient (Berner, 2004). It has been shown that vegetation
245 cover (*VC %*) has a negative exponential correlation with soil erosion rate (Gyssels et al.,
246 2005); i.e., $E_r \propto \exp(-b*VC)$, where b is an exponential constant. Modern Earth has
247 approximately 60% vegetation cover; whereas, none was present on the Archean Earth.
248 Absence of vegetation on the Archean Earth might compensate partially for the effect of low
249 plateau elevation.

250

251 **3. Methods and Materials**

252 *3.1 Chemical weathering model*

253 We modeled the chemical weathering of silicates using the geological carbon cycle
254 model of Krissansen-Totton et al. (2018), with two modifications. First, we used three models
255 for the emergence of land above sea level as introduced above rather than the estimates of
256 continental growth used in Krissansen-Totton et al. (2018). Second, because there was no

257 macroscopic vegetation on the Archean Earth, we set the vegetation compensating factor as
258 0.25 rather than 0.1 to 1, randomly sampled over the Precambrian in the original model. We
259 kept all other parameters as in the original code.

260 The dissolution rate of apatite (R) has been proposed (Guidry and Mackenzie, 2000)
261 to be:

262 $$R = A * \exp\left(-\frac{E_a}{R_g T}\right) * [H^+]^{n_H} \quad (1)$$

263 R: mole/(cm^2*s); A: reaction constant, mole/(cm^2*s); E_a: activation energy of dissolution
264 (34.7 kJ/mole) (Guidry and Mackenzie, 2003); R_g: universal gas constant, 0.008 kJ/(mole*K);
265 T: temperature, K; [H$^+$]: activity of hydrogen ion in the weathering fluid; n_H: reaction order
266 (0.81 at 2 < pH < 5.5) (Guidry and Mackenzie, 2003).

267 Eqn. 1 has been used to estimate continental inputs of P during the past 600 Ma (Guidry and
268 Mackenzie, 2000). Guidry and Mackenzie (2000) assumed a constant [H$^+$] of 10^{-5} for soil
269 waters throughout this interval; however, the log dissolution rate of apatite can decrease
270 linearly with pH at pH < 6 (Guidry and Mackenzie, 2003). Due to high levels of $CO_{2,g}$ in the
271 Archean atmosphere, weathering fluids would have been generally acidic (Hao et al., 2017a).
272 Thus,

273 $$\frac{R_{Archean}}{R_{Modern}} = \exp\left[-\frac{E_A}{R_g}\left(\frac{1}{T_{Archean}} - \frac{1}{T_{Modern}}\right)\right] * \left(\frac{H^+_{Archean}}{H^+_{Modern}}\right)^{n_H} \quad (2)$$

274 At acidic pH, [H$^+$] of rainwater varies approximately with the partial pressure of $CO_{2,g}$
275 ($P_{CO_{2,g}}$):

276 $$[H^+]^2 = K_1 * K_{CO_2} * P_{CO_{2,g}}$$

277 $$[H^+] = K * \sqrt{P_{CO_2}} \quad (3)$$

278 where $K = \sqrt{K_1 * K_{CO_2}}$; K_1 represents the first deprotonation constant of carbonic acid; K_{CO_2}
279 represents the solubility constant of $CO_{2,g}$ in water under ambient conditions.

It is notable that the pH of weathering fluids would have increased as weathering progressed due to release of alkalinity from the alteration of silicate and carbonate minerals. However, as shown in Hao et al. (2017a), the pH increment from rainwater (starting weathering fluid) to river water (ending weathering fluid) is similar at different levels of $pCO_{2,g}$; i.e. $\frac{H^+_{Archean}}{H^+_{Modern}}$ of weathering fluids should depend primarily on $\frac{pCO_{2,g,Archean}}{pCO_{2,g,Modern}}$. Apart from the dissolution of $CO_{2,g}$, introduction of organic acids as well as SO_x and NO_x gases may affect the acidity of rainwater, particularly in some local environments or during particular geologic periods. However, deposition of SO_x and NO_x, which are mostly anthropogenic today, might have been insignificant for the preindustrial times, let alone for the Archean Eon. The overall effects of organic acids, which mainly come from macroscopic vegetation today, were considered in our model as discussed below.

Consequently, the relative chemical weathering rate of apatite is

$$\frac{R_{Archean}}{R_{Modern}} = \exp\left[-\frac{E_A}{R_g}\left(\frac{1}{T_{Archean}} - \frac{1}{T_{Modern}}\right)\right] * \left(\frac{P_{CO_{2,Archean}}}{P_{CO_{2,Modern}}}\right)^{\frac{n_H}{2}} \quad (4)$$

Recently, Krissansen-Totton et al. (2018) reconstructed the evolution of Archean surface environments, including $pCO_{2,g}$ and temperature, based on a model for the geological carbon cycle. Here, we incorporate the weathering kinetics of apatite (eqn. 4) into Krissansen-Totton et al.'s model and use their output of $pCO_{2,g}$ and temperature of each run to calculate the weathering kinetics of phosphorus as it changed through the Archean Eon.

We developed three versions of our model, reflecting hypotheses for early, intermediate and late continental emergence (Fig. 1a). All generate results that are similar in trajectory, albeit different in timing. While the question of when and to what extent continents emerged above sea level remains a topic for debate, we believe there are compelling reasons to favor late emergence hypotheses, as proposed in models that relate the water cycle (Korenaga et al., 2017) and continental hypsometry (Rey and Colitce, 2008) to a

304 secular decline in mantle temperature through the Archean Eon. Based on sedimentary and
305 geochemical evidence (*Sec. 2.1*), we favor large-scale subaerial emergence of continents in
306 the late Archean Eon as the most likely scenario. As we discuss below (**Discussion**),
307 weathering of P on early and middle Archean continents might have also been suppressed by
308 slow physical erosion due to the low elevation of emergent land masses.

309 Lastly, vegetation has been shown to accelerate chemical weathering by a factor of
310 about 4 (Berner, 2004; Lenton et al., 2018); thus, the weathering kinetics of apatite are
311 divided by 4 to compensate for the effect of no vegetation in the Archean.

312 The total flux (p) of P by continental weathering is

313 $$p(t) = SA * R \quad (5)$$

314 SA: global surface area of apatite available for weathering.

315 Therefore,

316 $$\frac{p(Archean)}{p(Modern)} = \frac{SA_{Archean} * R_{Archean} * C(P)_{Archean}}{SA_{Modern} * R_{Modern} * C(P)_{Modern}} \quad (6)$$

317 $C(P)$: content of P in the rock. Here, the ratio of SA * C(P) was used to approximate the
318 relative exposure of apatite minerals for chemical weathering on exposed Archean and
319 modern continents.

320 For simplicity, we assumed an average P content for Archean land equal to half the
321 modern value, i.e. $C(P)_{Archean}/C(P)_{Modern} = 1/2$. This assumption is within the range of values
322 reported in Cox et al.'s compilation (Cox et al., 2018). Regardless of the uncertainties in this
323 estimate, we consider the evolution of crustal P content to be less important for the
324 continental transport of reactive P than weathering rate and continental growth and
325 emergence (Flament et al., 2013; Korenaga et al., 2017). As in Krissansen-Totton et al.
326 (2018), the weathering model was run 10,000 times to build distributions for model outputs.

327 Due to lack of a universal value for the weathering rate of apatite on the modern Earth,
328 we calculated only the relative weathering rate of apatite on the Archean Earth compared to

329 preindustrial time using Eqn. (4) (**Figs. 2-4**). Similarly, we calculated only the relative
330 chemical dissolution flux of P using Eqn. (6), due to the fact that the speciation of P in
331 reducing and acidic Archean river water might have differed substantially from that of
332 preindustrial rivers (*Sec. 4.2* and **Table 2**).
333
334 *3.2 Physical erosion*
335 As mentioned above, elevation and vegetation are two major factors controlling rates
336 of physical erosion:
337 $$\frac{E_{r,Archean}}{E_{r,Modern}} = \frac{H_{Archean}}{H_{Modern}} \times e^{-b(VC_{Archean} - VC_{Modern})} \quad (7)$$
338 Reported *b* values vary significantly and this variation strongly affects the calculated
339 effectiveness of vegetation on the protection of soil from erosion (Gyssels et al., 2005). Here,
340 we adopt a range of *b* values from 0.02 to 0.04, representing the range of literature values
341 (Gyssels et al., 2005). With no information of actual Archean plateau elevations, we chose to
342 apply Flament et al.'s (2013) reconstructed maximum plateau, which should approximate an
343 upper limit on actual elevations. The vegetation coverage in the Archean ($VC_{Archean}$) is set to
344 be 0 and modern (VC_{Modern}) to be 60%.
345
346 *3.3 Thermodynamic calculations of P-minerals' solubilities*
347 Solubility limits for primary and secondary phosphate minerals in Archean river water
348 and seawater were calculated using the equilibrium constants of their dissolution reactions
349 under ambient conditions (25 °C and 1 atm) (**Table 1**). Based on previous studies, we made
350 various assumptions about concentrations for ions other than phosphate.
351 For our reconstruction of Archean river water, F^- concentration was assumed to be
352 equal to that of modern river water; i.e., $1.3 * 10^{-8}$ mole/L (Deshmukh et al., 1995) although
353 the actual level is unknown. This simple consideration might over- or under-estimate the

354 solubility limits of F-bearing phosphates. However, our calculations suggest that the F-
355 bearing phosphates are highly soluble in the Archean weathering fluids (**Fig. 5a** and **b**) and
356 the results are still valid even with orders of magnitude higher or lower levels of fluorine.
357 Due to high levels of $CO_{2,g}$, Archean river water is expected to have been more acidic than at
358 present (Hao et al., 2017b). Acidity of the weathering fluid also depends on the extant of
359 reactions with silicate and carbonate minerals, increasing at high reaction extent due to the
360 release of alkalinity by rock alteration. Here, we investigated a wide range of Archean $pCO_{2,g}$
361 values (1 to $10^{-2.5}$ bar) from Krissansen-Totton et al. (2018) and modeled the corresponding
362 chemistry of Archean river water using a previously reported late Archean weathering model
363 (Hao et al., 2017b). The outputs, particularly pH and aqueous activity of Ca^{2+}, Fe^{2+}, Cl^-, and
364 $SiO_{2,aq}$ (**Table S1**), were used to calculate the solubilities of primary and secondary P-
365 minerals, based on the reported thermodynamics of these minerals (**Table 1**). As for the
366 solubilities of variscite ($AlPO_4 \cdot 2H_2O$) and strengite ($FePO_4 \cdot 2H_2O$), Al(III) and Fe(III) levels
367 were assumed to be limited by the solubility of their corresponding amorphous hydroxides.
368 However, $Fe(OH)_3$ is not believed to have precipitated widely during Archean weathering, as
369 supported by observations of Fe-depletion in Archean paleosols (Rye and Holland, 1998).
370 Therefore, the solubility of strengite, although calculated in this study, should serve only as a
371 lower limit on Archean river water.
372
373 *3.4 P-weathering in paleosol record*
374 Paleosol selection for our analysis is based mainly on standards proposed by Rye and
375 Holland (1998), augmented by more recent additions. **Table S2** lists all data sources.
376 The enrichment index of P is defined as:
377 $$\Delta\left(\frac{P}{Ti}\right) = \frac{\left(\frac{P}{Ti}\right)_{Paleosol} - \left(\frac{P}{Ti}\right)_{Bedrock}}{\left(\frac{P}{Ti}\right)_{Bedrock}} \quad (8)$$

Δ(P/Ti) > 0 indicates enrichment of P during weathering whereas Δ(P/Ti) < 0 indicates depletion of P. Since positive values of Δ(P/Ti) reflect the addition of P to the paleosols, most likely by mineral aerosols, we decided to use only negative Δ(P/Ti) values for Student's t-test (**Fig. 6**). **Fig. S4** presents all Δ(P/Ti) values and the corresponding statistical results.

4. Results

4.1 Continental weathering of phosphorus

As noted above, we have applied three cases of land emergence to simulate ratios of apatite dissolution rate (rate per unit area, e.g. mole/cm^2*s in this study; Figs. 2a-4a) and P weathering flux (Figs. 2b-4b) through the Archean Eon relative to modern.

In the case of slow late Archean emergence of land (Flament et al., 2013), the relative weathering rate of apatite decreases slowly but monotonically through the Archean Eon (**Fig. 2a**), largely due to the secular decline of $pCO_{2,g}$ (**Fig. S1**). When we compensate for a lack of vegetation, the apatite dissolution rate is always greater than five times the modern, indicating that dissolution of apatite was kinetically favorable under the acidic conditions of the Archean land surface. However, the relative weathering flux of P remains negligible until 3.5 Ga, when land starts to emerge and then increases rapidly (**Fig. 2b**), reaching a value ranging from 0.25 to 1 by the end of the Eon. The increase in weathering flux is largely ascribed to the late Archean emergence of land, which more than compensates for the declining weathering rate of apatite. However, continental weathering flux of silicates simulated by Krissansen-Totton et al. (2018) decreased slightly through the Archean Eon (Fig. 3E in Krissansen-Totten et al., 2018). This lack of synchronization is due to the different settings of land fraction (relative to the modern land area). In their simulations, Krissansen-Totton et al. (2018) assumed 0-75% land fraction emergence above sealevel and no change with time during the Archean Eon. Under these circumstances, decreasing $pCO_{2,g}$ and

403 temperature (Fig. 3B & D in Krissansen-Totten et al., 2018) would inevitably result in a
404 decreasing continental flux of silicate weathering. As argued by Krissansen-Totten et al.
405 (2018), the degree of land emergence has only a minor influence on the evolutionary history
406 of seawater pH and climate, the foci of their study. However, the geologic history of land
407 emergence as discussed in Sec. 2.1 is highly relevant to the estimation of continental
408 weathering flux. For this reason, we used reconstructed histories of Archean land emergence
409 (Fig. 1a) as inputs into our weathering model, which shows an increasing continental flux of
410 P through time. In **Fig. S1-3**, we also displayed our reconstructed evolution of continental
411 silicate weathering, which shows increasing flux as well, consistent with other geochemical
412 studies. These increasing fluxes of continental weathering are mainly driven by the land
413 emergence.

414 In the second case, where land emerged rapidly from the middle Archean (Korenaga
415 et al., 2017), the trends of relative weathering rate and flux are similar to the case described
416 above (**Fig. 3**). That said, the relative weathering rate of apatite decreases to even lower
417 levels toward the end of the Archean (**Fig. 3a**) compared with the slow emergence case. This
418 difference lies in the lower levels of $pCO_{2,g}$ and temperature, a consequence of stronger
419 continental weathering on a larger land surface in the late Archean Eon (**Fig. S2**). Similar to
420 the first case, the relative chemical weathering flux of P increases from the middle Archean
421 and reaches a value close to or higher than 1 by the end of the Archean, representing a flux
422 comparable to or higher than the modern value (**Fig. 3b**), again because of continental
423 emergence.

424 In the last case, where land started emerging early in the Archean Eon (Korenaga et
425 al., 2017), the relative weathering rate of apatite once again declines monotonically with time
426 (**Fig. 4a**). The relative weathering flux of P, however, increases rapidly from the early
427 Archean, reaching a plateau value of 0.5 to 4 in the middle Archean (3.5 Ga) before

decreasing slightly into the late Archean (**Fig. 4b**). This trend differs from two cases discussed above, mainly due to the rapid emergence of land in the early Archean. The declining weathering flux is largely ascribed to the declining weathering rate of apatite. In this case, the weathering flux of P is comparable to or higher than the modern level since the middle Archean. However, as mentioned earlier, we believe this case of early land emergence is not well supported by sedimentary and geochemical evidence. Additionally, on the early-middle Archean Earth, continental weathering, although chemically favorable, might have been severely limited by low rates of physical erosion, reflecting the low mean elevation of continental land (**Fig. 1b**), as elaborated in **Discussion**.

In summary, given three different cases of land emergence, Archean chemical weathering of apatite is always kinetically more favorable than today, and the weathering flux of P is predicted to have reached levels comparable to today at least by the end of the Archean Eon.

4.2 Riverine transport of phosphorus

Today, continental weathering of P-hosting minerals generates various forms of phosphorus. Among these, detrital particulate phosphorus is the largest component but is not biologically available to the marine ecosystem. Bioavailable phosphorus, also known as 'reactive' phosphorus, is composed of dissolved inorganic phosphorus (DIP), dissolved organic phosphorus (DOP), particulate organic phosphorus (POP), Fe-bound inorganic phosphorus (PIP, Fe-bound), and about 20% aeolian phosphorus (desorption from aeolian dusts) (Compton et al., 2000). The largest proportion of the reactive phosphorus pool is Fe-bound phosphorus, because during oxidative weathering Fe(II) is oxidized to Fe(III), leading to the formation of Fe(III)-(hydr)oxide or Fe(III)-coated clay minerals that have a high surface adsorption affinity for phosphate (House, 2003; Withers and Jarvie, 2008). This

surface retention of P is thought to be a key process limiting dissolved P levels in modern river water. However, in the Archean, when the atmosphere was anoxic and weakly reducing, weathering is thought to have leached Fe(II) without oxidation, as supported by the previously noted Fe-depletion in Archean paleosols (Rye and Holland, 1998). Therefore, we expect that there would have been little Fe-bound inorganic phosphate in Archean river water and, correspondingly, a higher concentration of dissolved inorganic phosphate (**Table 2**). Moreover, due to higher levels of atmospheric CO_2, Archean weathering fluids, including rainwater and river water, are thought to have been more acidic than today (Hao et al., 2017a). As presented in **Fig. 5a and b**, acidic and reducing Archean weathering fluids allow much higher solubilities of primary and secondary P-bearing minerals than dissolved P levels in modern river water at a wide range of pH values (4.5 – 7.5) (Gaillardet et al., 2014). Indeed, the dissolution of P-minerals in Archean acidic waters is both kinetically and thermodynamically more favorable than today. High solubility of phosphate in Archean river water would enable riverine transport of rapidly weathered phosphate to the sea(s).

Based on **Fig. 2b-4b**, the continental weathering flux of phosphorus in the late Archean was 0.3 to 3.5 times the modern value. In this study, we assumed that the total dissolved inorganic phosphate in Archean river water was the sum of modern DIP and Fe-bound PIP multiplied by the ratio of chemical weathering flux (p) between the Archean and modern (**Table 2**). Similarly, we assumed that chemical weathering of organic P from sedimentary rock (DOP and POP) and the physical weathering of phosphate (detrital and aeolian P) are influenced primarily by the relative weathering area (**Table 2**). However, this simple consideration might over- or under-estimate the contribution of these components. For example, physical weathering is dependent on many environmental factors, including elevation, climate, and vegetation (Drever, 1994; Edmond et al., 1995; Zhou et al., 2008). In the Archean, these all differed from today (see **Discussion**), complicating estimates of detrital

and aeolian P fluxes on the early Earth. Similarly, the weathering of organic P depends on a number of environmental factors, including the redox state of weathering fluids, the content of organic-P in sedimentary rock, and the presence of life. For example, organic matter should have had a longer retention time in anoxic Archean environments compared to today. Thus, organic P, once weathered, might have been stably transported in reducing Archean waters. Empirical analyses, however, show that the P content of Archean shales is lower than that of their modern counterparts (Reinhard et al., 2017). Regardless of these uncertainties, the contributions of organic and aeolian components to overall riverine fluxes would have been relatively small compared with the combined fluxes of dissolved inorganic and Fe-bound P. We note again that detrital P, although representing the largest proportion of continental P, is not biologically available. Therefore, we believe that our calculations provide a reasonable estimate of the continental input of bioavailable P to the Archean ocean.

Direct evidence of P-behaviors during Archean weathering comes from the paleosol record. The mobility of P in paleosols was assessed as the ratio of P to the immobile element Ti (relative to underlying bedrock) (**Methods and Materials**). To minimize the effect of post-depositional processes, we focused on long term trends in the mean level of P/Ti, a method applied widely in interpretations of ancient sediments (Cox et al., 2018; Planavsky et al., 2010; Stüeken et al., 2012). The result (**Fig. 6 & S4**) shows stronger depletion of P in Archean paleosols compared with younger examples. In addition, a Student's t-test of P/Ti in Archean and post-Archean paleosols confirms that Archean paleosols are significantly more depleted in P than their post-Archean counterparts ($p < 10^{-4}$) (**Fig. 6b & S4b**). These results are qualitatively coherent with the outputs of our weathering models, which indicate more pronounced weathering of P in the Archean relative to the modern Earth.

5. Discussion

503 Continental weathering is generally classified as either kinetically- or transport-
504 limited, depending on relative rates of chemical weathering and physical erosion (West et al.,
505 2005). For kinetically-limited weathering, the rate of physical erosion exceeds the rate of
506 chemical weathering; total weathering flux is then limited by the chemical weathering supply.
507 In the case of transport-limited weathering, the rate of chemical weathering depends on
508 exposure of fresh rock by physical erosion; total weathering flux is limited by the removal of
509 regolith by physical erosion. Climate and tectonics are two major factors controlling these
510 weathering scenarios.

511 Considering the high atmospheric $pCO_{2,g}$ of Archean Earth (Hart, 1978; Kasting et al.,
512 1989; Krissansen-Totton et al., 2018; Owen et al., 1979), chemical weathering of silicates
513 should have been more rapid than in the modern environment (Berner, 2004). In contrast,
514 physical erosion of Archean continents might have been limited by the restricted area and
515 low elevation of mountainous areas. Geophysical models indicate that hot Archean
516 continental lithosphere could not support mountains with high elevations (Flament et al.,
517 2013; Rey and Coltice, 2008). Specifically, the maximum elevation of continental plateaus
518 might have increased from around 1000 to 3900 m (**Fig. 1b**) as the mantle cooled through
519 Archean time, in contrast to 5500 m for present-day Tibet (Flament et al., 2013). The
520 elevation of mountainous areas has long been proposed to control maximum erosion fluxes
521 (Edmond et al., 1995). Vegetation cover is another important factor that strongly affects
522 erosion (Gyssels et al., 2005). In order to decipher whether Archean weathering was
523 kinetically or transport limited, we adopted models from the literature to quantify the relative
524 rates of silicate weathering and physical erosion (**Methods and Materials**).

525 The result (**Fig. 7**) shows an increasing rate of physical erosion but decreasing rate of
526 chemical weathering from the early to late Archean Eon. During the Archean, the maximum
527 elevation of mountainous areas increased through time, as did the total area of emergent crust

528 (Flament et al., 2013; Korenaga et al., 2017), resulting in enhanced physical erosion. At the
529 same time, declining $pCO_{2,g}$ and temperature would have led to decreasing rate of chemical
530 weathering. The absence of vegetation in the Archean could have strengthened physical
531 erosion because of the lack of sediment protection (Drever, 1994); on the other hand,
532 weakened chemical weathering (Berner, 2004) would have had the opposite effect. The no-
533 vegetation effect, however, remained constant throughout the Archean and, hence, makes no
534 contribution to rate changes within the Eon.

535 In all three scenarios, the system begins in a predominantly transport-limited regime
536 and transitions to one of largely kinetic limitation, with the time of cross-over depending on
537 the model for continental emergence. Thus, in our preferred scenario, high rates of chemical
538 weathering were favored by early and middle Archean conditions (**Fig. 2-4**), but continental
539 flux of P to the oceans would have been limited by slow physical erosion and the limited
540 exposure of fresh rock. It is notable that our model input of elevation represents the
541 maximum elevation of Archean plateaus reconstructed by Flament et al. (2013). The actual
542 elevation might have been much lower, indicating even slower erosion rates. As relative rates
543 of physical erosion increased, they came to exceed the relative rate of chemical weathering in
544 the late Archean (3.0 to 2.5 Ga) (**Fig. 7**). From then on, continental flux of P was dominated
545 by the flux of chemical weathering (**Fig. 2b-4b**). On the modern Earth silicate weathering is
546 transport-limited in catchments such as continental cratons while kinetically limited in alpine
547 and submontane catchments (West et al., 2005). On the global scale, Hartmann et al. (2014)
548 estimated the effect of soil on chemical weathering flux and suggested a 40 % reduction by
549 soil shielding compared to an Earth surface covered by young rocks. Nevertheless, our
550 calculated relative rate of physical erosion could exceed that of chemical weathering by
551 several-fold on the late Archean Earth (**Fig. 7**), marking a notable transition from large-scale
552 transport-limited weathering in the early and middle Archean to kinetically-limited

553 weathering in the late Archean Eon. This result confirms our flux calculations, which indicate
554 that continental weathering could have contributed comparable or higher amounts of
555 bioavailable phosphorus to the late Archean ocean ecosystem than occurs today.
556
557 **6. Conclusions**
558 Chemical weathering depends on several factors that have changed through time,
559 including temperature, pH, vegetation cover, and the chemical composition, exposed area,
560 and elevation of land masses. Given high but decreasing pCO_2 in the Archean atmosphere,
561 rates of apatite weathering should have been high early in the Archean and then decreasing
562 through the duration of the eon. Despite the high apatite weathering rates dictated by
563 relatively acidic rainwater, P fluxes from the continents to the oceans were probably very low
564 in the early Archean because of limitations in the exposed surface area and elevation of
565 continents. As continents emerged through time, P fluxes to the oceans would have increased,
566 reaching values comparable to the modern by the end of the eon.
567 We have modeled secular changes in P fluxes in relation to three distinct models for
568 continental emergence. Not surprisingly, they give results that differ in timing but agree in
569 overall trend. Increasingly, stratigraphic, geophysical, and geochemical data support strong
570 continental emergence in the late Archean Eon (Bindeman et al., 2018; Flament et al., 2013,
571 2008; Spencer et al., 2019), favoring a variant on the model results shown in **Figure 1**.
572 Depending on the exact time scale of continental emergence, the major increase in P flux to
573 the ocean could have occurred close to the Archean-Proterozoic boundary.
574 Such a history has a number of implications for primary production early in Earth
575 history. Among other things, the inferred time trajectory of P flux to the oceans lessens the
576 need for models that posit the evolution of oxygenic photosynthesis just before the Great
577 Oxidation Event at ca. 2.4 Ga. Even if oxygenic phototrophs (cyanobacteria) existed in early

578 Archean oceans, rates of primary production might have been too low to affect atmospheric
579 oxygenation. Also, above a critical level of Fe/P in the oceans, anoxygenic photoautotrophs
580 would have been favored ecologically over oxygenic photoautotrophs in most parts of the
581 Archean biosphere (Jones et al., 2015), which could account for the carbon mass balance
582 inferred from carbon isotopes (Krissansen-Totton et al., 2015) without producing O_2.
583 Transiently high oxygen production – and consequently, "oxygen oases" – would have been
584 possible locally where P availability was high and/or the availability of alternate electron
585 acceptors for photosynthesis was low. Molecular phylogenies that place the origin of
586 oxygenic photosynthesis in freshwater (Blank and Sanchez-Baracaldo, 2010) are consistent
587 with this reasoning and our model results. And, as others have argued (e.g., Flament et al.,
588 2008; Campbell and Davies, 2017), increased P fluxes associated with late Archean
589 continental emergence could have fueled the relatively high rates of oxygenic photosynthesis
590 needed to nudge Earth's surface into a permanently oxic state.

Acknowledgements We thank Dimitri A. Sverjensky, David Catling, Cin-Ty Lee, Nicolas Coltice, Ciaran Harman, Mathew Pasek, Michael Kipp, Lu Pan, and Chao Liu for helpful discussions, and two anonymous reviewers and Tim Lenton for constructive comments. JHH and ID thank French National Research Agency (#ANR-15-CE31-0010) and JHH, AHK, FH, and RMH thank W.M. Keck Foundation for financial supports.

Author contributions JHH and AHK conceived of the project. JHH compiled and FH analyzed the paleosol data. JHH and FH performed the simulations; JHH and AHK analyzed the results. All authors discussed the results and wrote the manuscript.

601

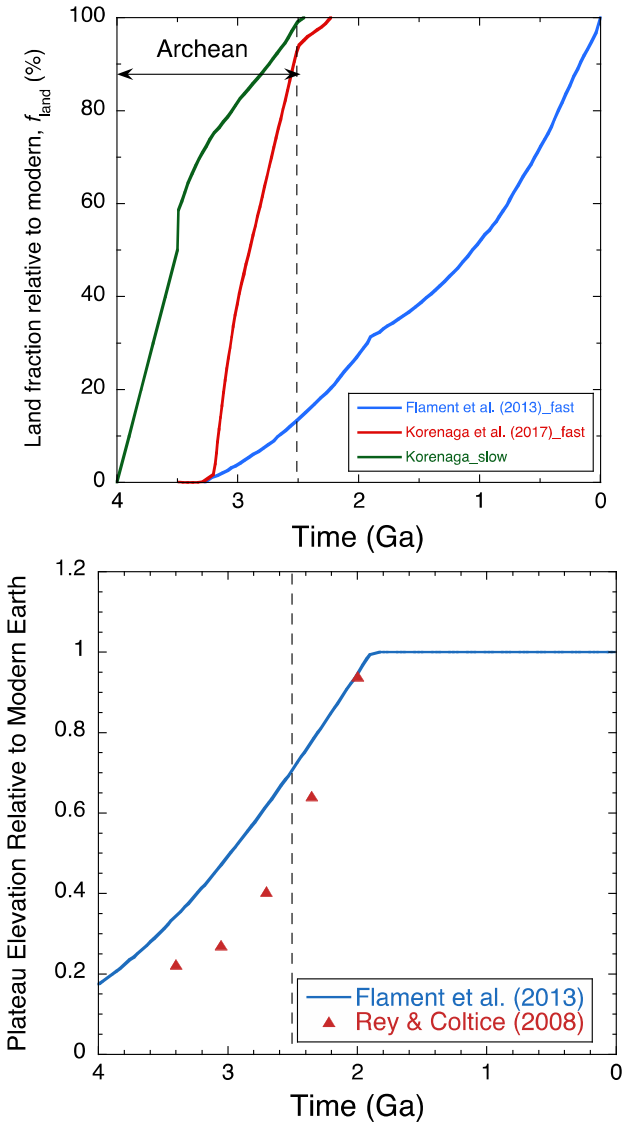

602

603 Figure 1. The timing of continental emergence: (a) emergence of continental land above sea
604 level according to Flament et al. (2013) and Korenaga et al. (2017) and (b) ratio of maximum
605 plateau elevation on the Archean Earth relative to today (5520 m).

606

607

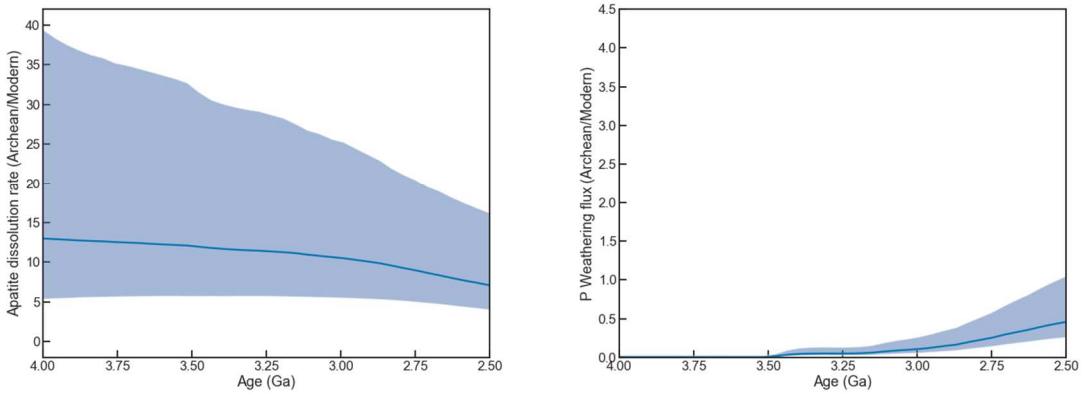

608

609 Figure 2. Continental weathering of phosphorus in the case of slow continental emergence in
610 the late Archean Eon (Flament et al., 2013, in Figure 1): (a) ratio of acidic dissolution rates of
611 apatite (rate per unit area) in the Archean relative to today; (b) ratio of weathering flux of
612 phosphorus in the Archean relative to today. Solid lines show median outputs, and shaded
613 regions show 95% confidence intervals.

614

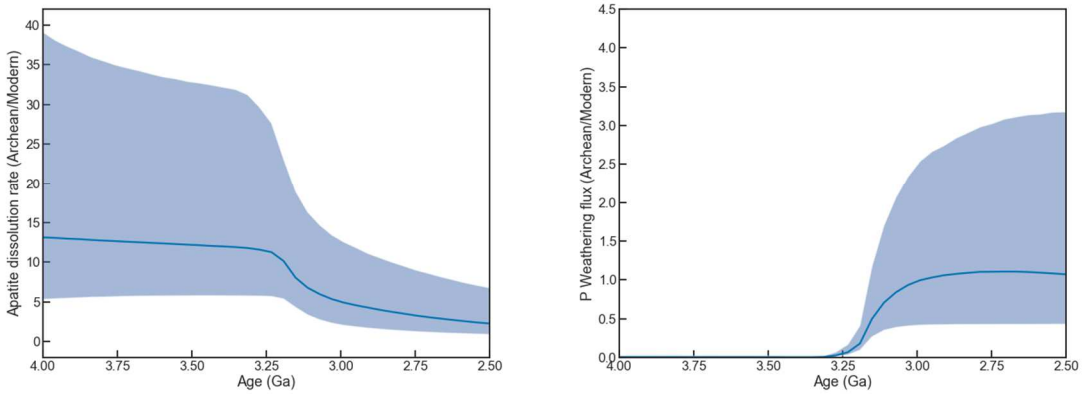

615

616 Figure 3. Continental weathering of phosphorus in the case of rapid continental emergence in
617 the late Archean (Korenaga et al., fast in Figure 1): (a) acidic dissolution rates of apatite
618 relative to today;(b) weathering flux of phosphorus relative to today. Solid lines show median
619 outputs, and shaded regions show 95% confidence intervals.

620

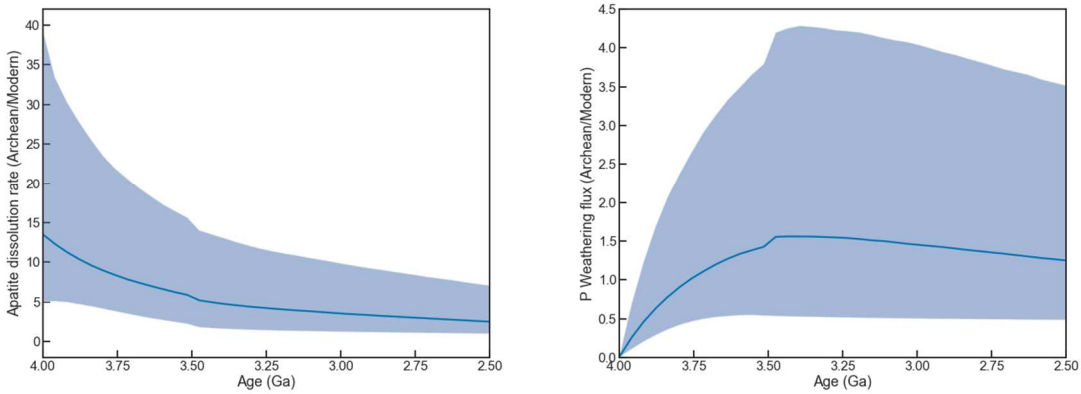

621

622 Figure 4. Continental weathering of phosphorus in the case of rapid continental emergence of
623 in the early Archean Eon (Korenaga_slow in Figure 1): (a) acidic dissolution rates of apatite;
624 (b) weathering flux of phosphorus. Solid lines show median outputs, and shaded regions
625 show 95% confidence intervals.

626

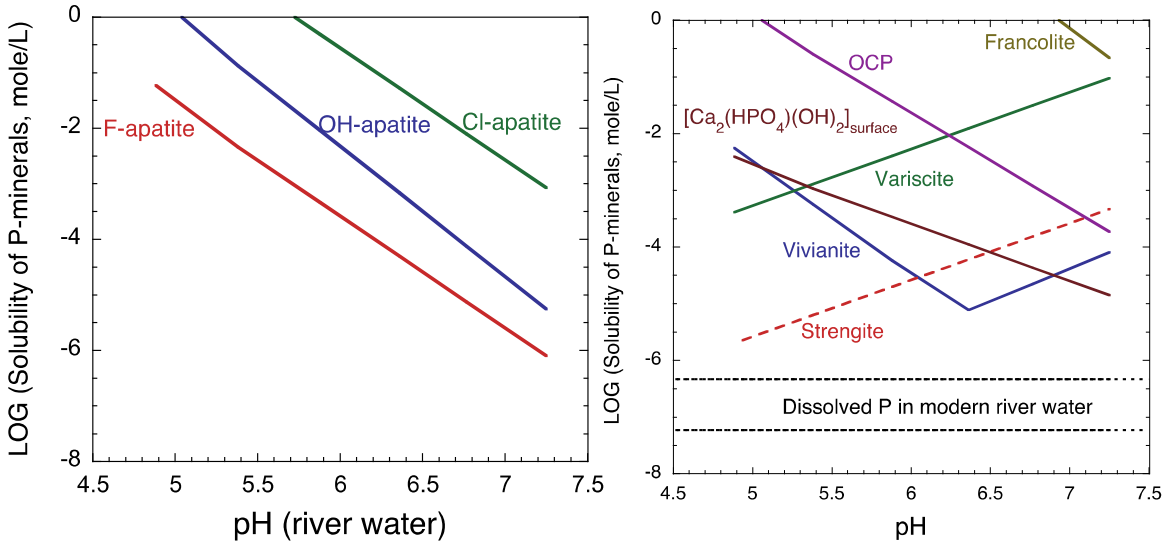

627

628 Figure 5. Leaching weathering of phosphorus on the Archean continents. (a) Solubility limits
629 of apatite in the Archean rainwater as a function of pH. (b) Solubility limits of various
630 secondary P-bearing minerals in Archean river water as a function of pH. See **Methods &**
631 **Materials** and **Table S1** for assumptions on the concentrations of other ions and **Table 1** for
632 thermodynamic data.

633

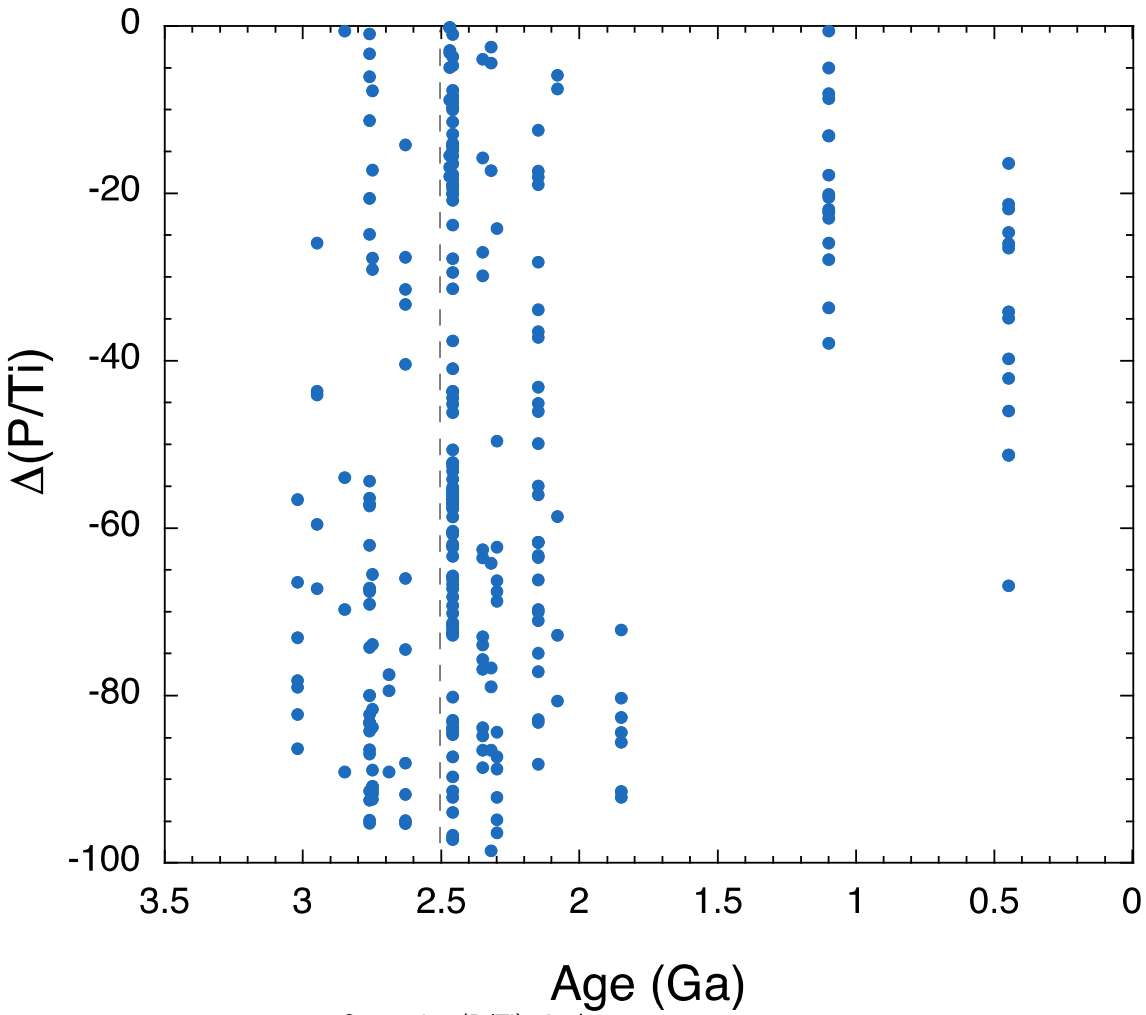

634

Group 1: (P/Ti)_Archean
Group 2: (P/Ti)_post-Archean

	Group 1	Group 2
Count	75	212
Mean	-63.9824	-48.2789
Variance	779.282	822.446
Std. Dev.	27.9156	28.6783
Std. Err	3.22342	1.96963

Mean Difference	-15.7035
Degrees of Freedom	133
t Value	-4.1571
t Probability	< .0001

635

636 Figure 6. Leaching weathering of P recorded in paleosols. (a) P depletion (ΔP/Ti < 0) relative
637 to bedrock in paleosols; (b) Student's t-test results of Archean and post-Archean paleosols'
638 ΔP/Ti.

639

640

641

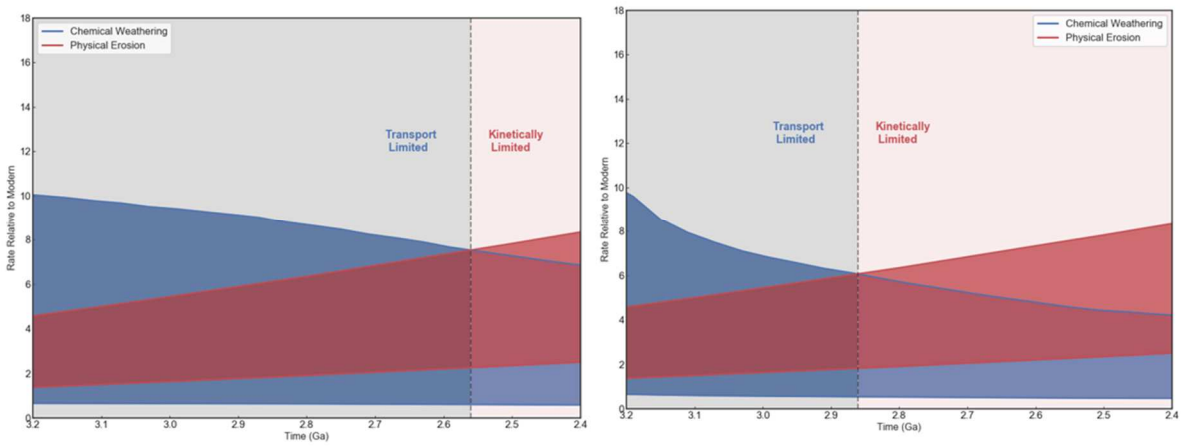

642

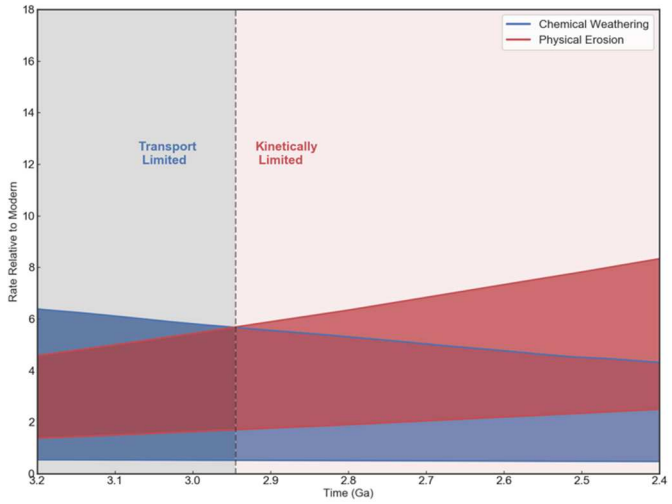

643 Figure 7. Relative intensity of chemical and physical weathering on the Archean Earth
644 compared with today in the three cases of continental emergence: (a) slow emergence in the
645 late Archean; (b) rapid emergence in the late Archean; (c) rapid emergence in the early
646 Archean. Blue shaded regions display 95% confidence intervals of the Archean silicate
647 weathering rate relative to today.

648

649 Table 1. Solubility reactions of primary and secondary P-bearing minerals in Archean river water.

Solubility in river water	Combined reaction[a]	Log K
OH-apatite	$Ca_5(PO_4)_3(OH) + 7H^+ \rightarrow 5Ca^{2+} + 3H_2PO_4^- + H_2O$	16.5 [a]
Cl-apatite	$Ca_5(PO_4)_3Cl + 6H^+ \rightarrow 5Ca^{2+} + 3H_2PO_4^- + Cl^-$	12.0 [a]
F-apatite	$Ca_5(PO_4)_3F + 6H^+ \rightarrow 5Ca^{2+} + 3H_2PO_4^- + F^-$	-1.15 [a]
Vivianite	$Fe_3(PO_4)_2*8H_2O + 4H^+ \rightarrow 3Fe^{2+} + 2H_2PO_4^- + 8H_2O$	3.31 [b]
Variscite	$AlPO_4{\cdot}2H_2O_{,s} + H_2O \rightarrow Al(OH)_{3,am} + H_2PO_4^- + H^+$	-8.27 [c]
Strengite	$FePO_4{\cdot}2H_2O,s + H_2O \rightarrow Fe(OH)_{3,am} + H_2PO_4^- + H^+$	-10.6 [d]
$[Ca_2(HPO_4)(OH)_2]_{surface}$	$Ca_5(PO_4)_3(OH) + 3H_2O + H^+ \rightarrow 2Ca_2(HPO_4)(OH)_2 + Ca^{2+} + H_2PO_4^-$	-2.59 [e]
Octacalcium phosphate (OCP)	$Ca_4H(PO_4)_3*2.5H_2O + 5H^+ \rightarrow 4Ca^{2+} + 3H_2PO_4^- + 2.5H_2O$	10.3 [f]
Francolite	$Ca_{10}(PO_4)_{5.5}(CO_3)_{0.5}F_{2.5} + 12H^+ \rightarrow 10Ca^{2+} + 5.5H_2PO_4^- + 0.5CO_{2,g} + 2.5\ F^- + 0.5H_2O$	38.0 [g]

650 [a]Calculated with SUPCRT92b (Johnson et al., 1992); [b]Calculated with SUPCRT92 and the reported log $K_{sp,Vivianite}$ (Al-Borno and Tomson,
651 1994); [c]Calculated with SUPCRT92b and the reported log $K_{sp,Variscite}$ (Stumm and Morgan, 1996); [d]Calculated with SUPCRT92b, log $K_{s,Fe(OH)3}$
652 (Liu and Millero, 1999), and the reported log $K_{sp,Strengite}$ (Stumm and Morgan, 1996); [e]Calculated with SUPCRT92b and data from (Fox et al.,
653 1985); [f]Calculated with SUPCRT92b and data from log $K_{sp,OCP}$ (Tung et al., 1988); [g]Calculated with SUPCRT92b and data from log $K_{sp,Francolite}$
654 (Vieillard, 1978).

655 Table 2. The continental flux of biologically available P (= DIP + DOP + POP + PIP Fe-
656 bound + 20% Aeolian) (Compton et al., 2000) in the late Archean compared with
657 preindustrial time (in 10^{10} moles P/yr).

Riverine Phosphorus	**Preindustrial**	**Late Archean**	**Bioavailability**
DIP (dissolved inorganic P)	0.97-1.6	1.5-30[a]	Y
DOP (dissolved organic P)	0.65	0.1-0.65[b]	Y
POP (particulate organic P)	2.9	0.3-2.9[c]	Y
PIP (particulate inorganic P), Fe-bound	4.8-9.7	0	Y
PIP, detrital	22-39	2.2-39[d]	N
Aeolian phosphorus	3.2	0.3-3.2[e]	20%[f]
Total (bioavailable P)	10-15.5	4-34	

658 [a](DIP(modern) + PIP,Fe-bound (modern)) * p(Archean)/p(Modern); [b]DOP(modern) *
659 SA(Archean)/SA(Modern); [c]POP(modern) * SA(Archean)/SA(Modern);
660 [d]PIP,detrital(Modern) * SA(Archean)/SA(Modern); [e]Aeolian(modern) *
661 SA(Archean)/SA(Modern); [f]Assume same percentage on the Archean Earth.
662

663 **References:**

664 Al-Borno, A., Tomson, M.B., 1994. The temperature dependence of the solubility product
665 constant of vivianite. Geochim. Cosmochim. Acta. **58(24)**, 5373-5378.
666 doi:10.1016/0016-7037(94)90236-4

667 Arndt, N., 1999. Why was flood volcanism on submerged continental platforms so common
668 in the Precambrian? Precambrian Res. **97(3-4)**, 155-164. doi:10.1016/S0301-
669 9268(99)00030-3

670 Bataille C. P., Willis A., Yang X. and Liu X. M. (2017) Continental igneous rock
671 composition: A major control of past global chemical weathering. *Sci. Adv.* **3**. Available
672 at: https://advances.sciencemag.org/content/3/3/e1602183.

673 Berner, R.A., 2004. The Phanerozoic Carbon Cycle: CO_2 and O_2. Oxford University Press
674 Oxford.

675 Berner E. K., Berner R. A. and Moulton K. L. (2003) Plants and Mineral Weathering: Present
676 and Past. In *Treatise on Geochemistry* pp. 169–188.

677 Bindeman, I.N., Zakharov, D.O., Palandri, J., Greber, N.D., Dauphas, N., Retallack, G.J.,
678 Hofmann, A., Lackey, J.S., Bekker, A., 2018. Rapid emergence of subaerial landmasses
679 and onset of a modern hydrologic cycle 2.5 billion years ago. Nature **557**, 545–548.
680 doi:10.1038/s41586-018-0131-1

681 Bjerrum, C.J., Canfield, D.E., 2002. Ocean productivity before about 1.9 Gyr ago limited by
682 phosphorus adsorption onto iron oxides. Nature **417**, 159–162. doi:10.1038/417159a

683 Blank, C.E., Sanchez-Baracaldo, P., 2010. Timing of morphological and ecological
684 innovations in the cyanobacteria - A key to understanding the rise in atmospheric
685 oxygen. Geobiology **8**, 1–23. doi:10.1111/j.1472-4669.2009.00220.x

686 Bluth G. J. S. and Kump L. R. (1991) Phanerozoic paleogeology. *Am. J. Sci.* **291**, 284–308.

687 Byerly, B.L., Lowe, D.L., Drabon, N., Coble, M.A., Burns, D.H., and Byerly, G.R., 2018.

688 Hadean zircon from a 3.3 Ga sandstone, Barberton greenstone belt, South Africa.
689 Geology **46**, 967-970. doi.org /10.1130 /G45276 .1
690 Campbell, I.H., Davies, D.R., 2017. Raising the continental crust. Earth Planet. Sci. Lett. **460**,
691 112-122. doi:10.1016/j.epsl.2016.12.011
692 Compton, J., Mallinson, D., Glenn, C.R., Filippelli, G., Föllmi, K., Shields, G., Zanin, Y.,
693 2000. Variations in the Global Phosphorus Cycle. Mar. Authigenes. From Glob. to
694 Microb. 21–33. doi:10.2110/pec.00.66.0021
695 Cox, G.M., Lyons, T.W., Mitchell, R.N., Hasterok, D., Gard, M., 2018. Linking the rise of
696 atmospheric oxygen to growth in the continental phosphorus inventory. Earth Planet. Sci.
697 Lett. **489**, 28–36. doi:https: 10.1016/j.epsl.2018.02.016
698 Culling W. E. H. (1960) Analytical Theory of Erosion. *J. Geol.* **68**, 336–344.
699 Culling W. E. H. (1963) Soil Creep and the Development of Hillside Slopes. *J. Geol.* **71**,
700 127–161.
701 Derry, L.A., 2015. Causes and consequences of mid-Proterozoic anoxia. Geophys. Res. Lett.
702 **42(20)**, 8538-8546 doi:10.1002/2015GL065333
703 Deshmukh, A.N., Wadaskar, P.M., Malpe, D.B., 1995. Fluorine in environment: A review.
704 Gondwana Geol. Mag **9**, 1–20.
705 Drabon N., Lowe D. R., Byerly G. R. and Harrington J. A. (2017) Detrital zircon
706 geochronology of sandstones of the 3.6-3.2 Ga Barberton greenstone belt: No evidence
707 for older continental crust. *Geology* **45**, 803–806.
708 Drever, J.I., 1994. The effect of land plants on weathering rates of silicate minerals. Geochim.
709 Cosmochim. Acta. **58(10)**, 2325-2332. doi:10.1016/0016-7037(94)90013-2
710 Edmond, J.M., Palmer, M.R., Measures, C.I., Grant, B., Stallard, R.F., 1995. The fluvial
711 geochemistry and denudation rate of the Guayana Shield in Venezuela, Colombia, and
712 Brazil. Geochim. Cosmochim. Acta **59**, 3301–3325. doi:10.1016/0016-7037(95)00128-

M

Ernst, W.G., Sleep, N.H., Tsujimori, T., 2016. Plate-tectonic evolution of the Earth: bottom-up and top-down mantle circulation. Can. J. Earth Sci. **53(11)**, 1103-1120. doi:10.1139/cjes-2015-0126

Flament, N., Coltice, N., Rey, P.F., 2013. The evolution of the87Sr/86Sr of marine carbonates does not constrain continental growth. Precambrian Res. **229**, 177–188. doi:10.1016/j.precamres.2011.10.009

Flament, N., Coltice, N., Rey, P.F., 2008. A case for late-Archaean continental emergence from thermal evolution models and hypsometry. Earth Planet. Sci. Lett. **275(3-4)**, 326-336. doi:10.1016/j.epsl.2008.08.029

Fox, L.E., Sager, S.L., Wofsy, S.C., 1985. Factors controlling the concentrations of soluble phosphorus in the Mississippi estuary. Limnol. Oceanogr. **30(4)**, 826-832. doi:10.4319/lo.1985.30.4.0826

Gaillardet, J., Viers, J., Dupré, B., 2014. 7.7 - Trace Elements in River Waters A2 - Turekian, Heinrich D. HollandKarl K, in: Treatise on Geochemistry (Second Edition). Elsevier, Oxford, pp. 195–235. doi:http://dx.doi.org/10.1016/B978-0-08-095975-7.00507-6

Gough, D.O., 1981. Solar interior structure and luminosity variations. Sol. Phys. **74**, 21–34. doi:10.1007/BF00151270

Guidry, M.W., Mackenzie, F.T., 2003. Experimental study of igneous and sedimentary apatite dissolution: Control of pH, distance from equilibrium, and temperature on dissolution rates. Geochim. Cosmochim. Acta. **67(16)**, 2949-2963. doi:10.1016/S0016-7037(03)00265-5

Guidry, M.W., Mackenzie, F.T., 2000. Apatite weathering and the Phanerozoic phosphorus cycle. Geology **28**, 631–634. doi: 10.1130/0091-7613(2000)028<0631:Awatpp>2.3.Co;2

738 Gyssels, G., Poesen, J., Bochet, E., Li, Y., 2005. Impact of plant roots on the resistance of
739 soils to erosion by water: A review. Prog. Phys. Geogr. **29(2)**, 189-217.
740 doi:10.1191/0309133305pp443ra
741 Hao, J., Sverjensky, D.A., Hazen, R.M., 2019. Redox states of Archean surficial
742 environments: The importance of $H_{2,g}$ instead of $O_{2,g}$ for weathering reactions. Chem.
743 Geol. **521**, 49-58. doi:10.1016/j.chemgeo.2019.05.022
744 Hao, J., Sverjensky, D.A., Hazen, R.M., 2017a. Mobility of nutrients and trace metals during
745 weathering in the late Archean. Earth Planet. Sci. Lett. **471**, 148–159.
746 doi:10.1016/j.epsl.2017.05.003
747 Hao, J., Sverjensky, D.A., Hazen, R.M., 2017b. A model for late Archean chemical
748 weathering and world average river water. Earth Planet. Sci. Lett. **457**, 191–203.
749 doi:10.1016/j.epsl.2016.10.021
750 Hart M. H. (1978) The evolution of the atmosphere of the earth. *Icarus* **33**, 23–39.
751 Hartmann J., Moosdorf N., Lauerwald R., Hinderer M. and West A. J. (2014) Global
752 chemical weathering and associated p-release - the role of lithology, temperature and
753 soil properties. *Chem. Geol.* **363**, 145–163.
754 Hawkesworth, C.J., Kemp, A.I.S., 2006. Evolution of the continental crust. Nature.
755 **443(7113)**, 811. doi:10.1038/nature05191
756 House, W.A., 2003. Geochemical cycling of phosphorus in rivers. Appl. Geochemistry **18**,
757 739–748. doi:10.1016/S0883-2927(02)00158-0
758 Jadamec M. A., Turcotte D. L. and Howell P. (2007) Analytic models for orogenic collapse.
759 *Tectonophysics* **435**, 1–12.
760 Johnson, J.W., Oelkers, E.H., Helgeson, H.C., 1992. SUPCRT92: A software package for
761 calculating the standard molal thermodynamic properties of minerals, gases, aqueous
762 species, and reactions from 1 to 5000 bar and 0 to 1000 °C. Comput. Geosci. **18**, 899–

947. doi:10.1016/0098-3004(92)90029-Q

Jones, C., Nomosatryo, S., Crowe, S.A., Bjerrum, C.J., Canfield, D.E., 2015. Iron oxides, divalent cations, silica, and the early earth phosphorus crisis. Geology **43**, 135–138. doi:10.1130/G36044.1

Kasting J. F., Zahnle K. J., Pinto J. P. and Young A. T. (1989) Sulfur, ultraviolet radiation, and the early evolution of life. *Orig. Life Evol. Biosph.* **19**, 95–108.

Kipp, M.A., Stüeken, E.E., 2017. Biomass recycling and Earth's early phosphorus cycle. Sci. Adv. 3. doi:10.1126/sciadv.aao4795

Knoll A. H. and Beukes N. J. (2009) Introduction: Initial investigations of a Neoarchean shelf margin-basin transition (Transvaal Supergroup, South Africa). *Precambrian Res.* **169**, 1–14.

Korenaga, J., Planavsky, N.J., Evans, D.A.D., 2017. Global water cycle and the coevolution of the Earth's interior and surface environment. Philos. Trans. R. Soc. A Math. Phys. Eng. Sci. **375(2094)**:20150393.. doi:10.1098/rsta.2015.0393

Krissansen-Totton, J., Arney, G.N., Catling, D.C., 2018. Constraining the climate and ocean pH of the early Earth with a geological carbon cycle model. Proc. Natl. Acad. Sci. 201721296. doi:10.1073/pnas.1721296115

Krissansen-Totton, J., Buick, R., Catling, D.C., 2015. A statistical analysis of the carbon isotope record from the Archean to phanerozoic and implications for the rise of oxygen. Am. J. Sci. **315(4)**, 275-316. doi:10.2475/04.2015.01

Kump, L.R., Barley, M.E., 2007. Increased subaerial volcanism and the rise of atmospheric oxygen 2.5 billion years ago. Nature. **448(7157)**, 1033. doi:10.1038/nature06058

Laakso, T.A., Schrag, D.P., 2018. Limitations on Limitation. Global Biogeochem. Cycles **32**, 486–496. doi:10.1002/2017GB005832

Lee, C.-T.A., Thurner, S., Paterson, S., Cao, W., 2015. The rise and fall of continental arcs:

Interplays between magmatism, uplift, weathering, and climate. Earth Planet. Sci. Lett. **425**, 105–119. doi:10.1016/j.epsl.2015.05.045

Lee, C.T.A., Caves, J., Jiang, H., Cao, W., Lenardic, A., McKenzie, N.R., Shorttle, O., Yin, Q. zhu, Dyer, B., 2018. Deep mantle roots and continental emergence: implications for whole-Earth elemental cycling, long-term climate, and the Cambrian explosion. Int. Geol. Rev. **60(4)**, 431-448. doi:10.1080/00206814.2017.1340853

Lenton T. M., Daines S. J. and Mills B. J. W. (2018) COPSE reloaded: An improved model of biogeochemical cycling over Phanerozoic time. *Earth-Science Rev.* **178**, 1–28.

Liu, X., Millero, F.J., 1999. The solubility of iron hydroxide in sodium chloride solutions. Geochim. Cosmochim. Acta. **63(19-20)**, 3487-3497. doi:10.1016/S0016-7037(99)00270-7

Lowe D. R. and Byerly G. R. (1999) *Geologic evolution of the Barberton greenstone belt, South Africa*., Geological Society of America.

Marks, M.A.W., Markl, G., 2017. A global review on agpaitic rocks. Earth-Science Rev. **173**, 229-258. doi:10.1016/j.earscirev.2017.06.002

Molnar, P., 2018. Gravitational Potential Energy per Unit Area as a Constraint on Archean Sea Level. Geochemistry, Geophys. Geosystems. **19(10)**, 4063-4095. doi:10.1029/2018GC007766

Neaman, A., Chorover, J., Brantley, S.L., 2005. Element mobility patterns record organic ligands in soils on early Earth. Geology **33**, 117–120. doi:10.1130/G20687.1

Nocita B. W. (1989) Sandstone petrology of the Archean Fig Tree Group, Barberton greenstone belt, South Africa: tectonic implications. *Geology* **17**, 953–956.

Owen T., Cess R. D. and Ramanathan V. (1979) Enhanced CO2 greenhouse to compensate for reduced solar luminosity on early Earth [5]. *Nature* **277**, 640–642.

Pasek, M., Lauretta, D., 2008. Extraterrestrial flux of potentially prebiotic C, N, and P to the

early earth. Orig. Life Evol. Biosph. **38(1)**, 5-21. doi:10.1007/s11084-007-9110-5

Planavsky, N.J., Rouxel, O.J., Bekker, A., Lalonde, S. V, Konhauser, K.O., Reinhard, C.T., Lyons, T.W., 2010. The evolution of the marine phosphate reservoir. Nature **467**, 1088–1090. doi:10.1038/nature09485

Pons, M.L., Fujii, T., Rosing, M., Quitté, G., Télouk, P., Albarède, F., 2013. A Zn isotope perspective on the rise of continents. Geobiology. **11(3)**, 201-214. doi:10.1111/gbi.12030

Porder, S., Ramachandran, S., 2013. The phosphorus concentration of common rocks-a potential driver of ecosystem P status. Plant Soil. **367(1-2)**, 41-55. doi:10.1007/s11104-012-1490-2

Reinhard, C.T., Planavsky, N.J., Gill, B.C., Ozaki, K., Robbins, L.J., Lyons, T.W., Fischer, W.W., Wang, C., Cole, D.B., Konhauser, K.O., 2017. Evolution of the global phosphorus cycle. Nature **541**, 386–389. doi:10.1038/nature20772

Rey, P.F., Coltice, N., 2008. Neoarchean lithospheric strengthening and the coupling of Earth's geochemical reservoirs. Geology **36**, 635–638. doi:10.1130/G25031A.1;

Roberts, N.M.W., Spencer, C.J., 2015. The zircon archive of continent formation through time. Geol. Soc. London, Spec. Publ. **389(1)**, 197-225. doi:10.1144/SP389.14

Ronov A. B. (1982) The Earth's Sedimentary Shell (Quantitative Patterns of its Structure, Compositions, and Evolution): The 20th V.l. Vernadskiy Lecture, March 12,1978. *Int. Geol. Rev.* **24**, 1313–1363.

Ruttenberg, K.C., 2013. The Global Phosphorus Cycle, in: Treatise on Geochemistry: Second Edition. doi:10.1016/B978-0-08-095975-7.00813-5

Rye, R., Holland, H.D., 1998. Paleosols and the evolution of atmospheric oxygen: A critical review. Am. J. Sci. **298**, 621–672. doi:10.2475/ajs.298.8.621

Satkoski, A.M., Lowe, D.R., Beard, B.L., Coleman, M.L., Johnson, C.M., 2016. A high

continental weathering flux into Paleoarchean seawater revealed by strontium isotope analysis of 3.26 Ga barite. Earth Planet. Sci. Lett. **454**, 28-35. doi:10.1016/j.epsl.2016.08.032

Schlesinger, W.H., Bernhardt, E.S., 2013. Biogeochemistry: an analysis of global change. Academic press.

Spencer, C.J., Partin, C.A., Kirkland, C.L., Raub, T.D., Liebmann, J., Stern, R.A., 2019. Paleoproterozoic increase in zircon $\delta^{18}O$ driven by rapid emergence of continental crust. Geochim. Cosmochim. Acta. **257**, 16-25. doi:10.1016/j.gca.2019.04.016

Stüeken, E.E., Catling, D.C., Buick, R., 2012. Contributions to late Archaean sulphur cycling by life on land. Nat. Geosci. **5**, 722–725. doi:10.1038/ngeo1585

Stumm, W., Morgan, J.J., 1996. Aquatic Chemistry: Chemical Equilibria and Rates in Natural Waters, 3rd edition. Wiley.

Taylor S. R. and McLennan S. M. (1985) The continental crust: Its composition and evolution., Blackwell Scientific Pub.,Palo Alto, CA, United States.

Trower, E.J., Lowe, D.R., 2016. Sedimentology of the ~3.3 Ga upper Mendon Formation, Barberton Greenstone Belt, South Africa. Precambrian Res. **281**, 473-494. doi:10.1016/j.precamres.2016.06.003

Tsukamoto, Y., Kakegawa, T., Graham, U., Liu, Z.-K., Ito, A., Ohmoto, H., 2018. Discovery of Ni-Fe Phosphides in the 3.46 Ga-Old Apex Basalt: Implications on the Phosphate Budget of the Archean Oceans. Goldschmidt Abstr. 2577.

Tung, M.S., Eidelman, N., Sieck, B., Brown, W.E., 1988. Octacalcium Phosphate Solubility Product from 4 to 37 °C. J. Res. Natl. Bur. Stand. **93**, 613-624. doi:10.6028/jres.093.153

Tyrrell T. (1999) The relative influences of nitrogen and phosphorus on oceanic primary production. *Nature* **400**, 525–531.

Van Kranendonk, M., 2006. Volcanic degassing, hydrothermal circulation and the flourishing

of early life on Earth: A review of the evidence from c. 3490-3240 Ma rocks of the Pilbara Supergroup, Pilbara Craton, Western Australia. Earth-Sci. Rev. **74**, 197– 240. doi:10.1016/j.earscirev.2005.09.005

Viehmann, S., Bau, M., Hoffmann, J.E., Münker, C., 2018. Decoupled Hf and Nd isotopes in suspended particles and in the dissolved load of Late Archean seawater. Chem. Geol. **483**, 111-118. doi:10.1016/j.chemgeo.2018.01.017

Vieillard, P., 1978. Géochimie des phosphates. Étude thermodynamique. Application à la genèse et à l'altération des apatites. Persée-Portail des revues scientifiques en SHS.

West, J., Galy, A., Bickle, M., 2005. Tectonic and climatic controls on silicate weathering. Earth Planet. Sci. Lett. **235**, 211–228. doi:10.1016/j.epsl.2005.03.020

Withers, P.J.A., Jarvie, H.P., 2008. Delivery and cycling of phosphorus in rivers: A review. Sci. Total Environ. **400(1-3)**, 379-395. doi:10.1016/j.scitotenv.2008.08.002

Zhou, P., Luukkanen, O., Tokola, T., Nieminen, J., 2008. Effect of vegetation cover on soil erosion in a mountainous watershed. Catena **75**, 319–325. doi:10.1016/j.catena.2008.07.010